THE ASTROPHYSICAL JOURNAL, 301:262–274, 1986 February 1

AN *EXOSAT* OBSERVATION OF QUIESCENT AND FLARE CORONAL X-RAY EMISSION FROM ALGOL

N. E. WHITE,[1,2] J. L. CULHANE,[3] A. N. PARMAR,[1,2] B. J. KELLETT,[3]
S. KAHN,[3] G. H. J. VAN DEN OORD,[4] AND J. KUIJPERS[4]
Received 1985 April 8; accepted 1985 July 31

ABSTRACT

X-ray emission from the Algol system is believed to originate in a corona associated with the K star. We have used the *EXOSAT Observatory* to make a 35 hr continuous observation centered on the occultation of the K star by the B star primary in order to investigate the spatial structure of the corona. The spectrum of the quiescent emission in the 1–10 keV band gives a temperature of 2.5×10^7 K. This spectrum, extrapolated to lower energies, can account for more than 80% of the observed count rate. No obvious X-ray eclipse was seen indicating the scale height of the 2.5×10^7 K component to be comparable to or greater than the radius of the underlying K star. An X-ray flare was detected with a rise time of ~ 1700 s and an exponential decay of ~ 7000 s. The 0.1–10 keV peak luminosity was 1.4×10^{31} ergs s^{-1}, 3 times more than the quiescent value. The peak temperature was 6×10^7 K, with an iron K line confirming the thermal character of the emission. A comparison of the flare parameters with possible cooling laws suggests that radiation cooling dominated and that the flare occurred in a loop with a height of 0.1–0.2 $R_\odot$. This loop was probably part of the complex responsible for a 7×10^6 K quiescent component reported by Swank and White in 1980.

Subject headings: stars: coronae — stars: eclipsing binaries — stars: individual — stars: X-rays — X-rays: binaries

I. INTRODUCTION

The coronal X-ray emission from stars with substantial convection zones (later than F) is, by analogy with the Sun, thought to originate in hot plasma contained in magnetic loop structures. The quiescent luminosity of the solar corona of $\sim 10^{26}$ ergs s^{-1} lies at the lower end of the observed range of quiescent stellar coronal luminosities which can reach up to a few times 10^{30} ergs s^{-1} (cf. Pallavicini *et al.* 1981). A strong correlation of X-ray luminosity with stellar rotation suggests that the enhanced stellar luminosities are caused by increased dynamo activity (Walter and Bowyer 1981; Pallavicini *et al.* 1981). In using the solar corona as a basis for understanding stellar coronae in general, it is important to establish how the solar model should be scaled to give the enhanced luminosities seen from the rapidly rotating stars.

Several approaches have been taken to investigate the various possibilities. Spectral measurements allow the emission measure and temperature of the plasma to be deduced and can be used to estimate the dimensions of the loops for an assumed coronal filling factor and loop pressure. The spectral observations which have been restricted to the brightest, usually more luminous systems (mainly the RS CVn binaries) show that in the 0.5–4.5 keV band, the coronal emission has two components with temperatures $\sim 7 \times 10^6$ K and $\sim 4 \times 10^7$ K (Holt *et al.* 1979; Swank *et al.* 1981). Both temperatures are higher than for the quiescent Sun and when the observed emission measures for both components are also considered, it is clear that either the pressure or the volume of the loops (or both) must be larger than in the solar case. When an X-ray flare is detected and its peak emission measure and temperature are obtained, the decay time can be equated to a cooling law to solve for the density and volume of the flaring loop (Haisch 1983; Stern, Underwood, and Antiochos 1983; Pye and McHardy 1983). While in the past the measured flare parameters have not been very restrictive, they have given volumes for the flaring region at least a factor of 100 larger than solar values.

The most direct approach is to combine the spectral measurements with an observation that includes an eclipse of the corona by a companion star, or a self-eclipse by the star itself, such that the spatial extent can be directly measured. Since the binary periods of many of the suitable systems are of the order of days, this requires a considerable investment in observing time, and up to now only two such measurements have been made; both of the same RS CVn system, AR Lac. From observations interspersed around one binary cycle of AR Lac, Walter, Gibson, and Basri (1983, hereafter WGB) found evidence for X-ray eclipses both at primary and secondary minima and from the depth and shape of the eclipses, they deduced for both stars typical coronal scale heights of $\sim 3 \times 10^9$ cm, with some evidence for a second $\sim 10^{11}$ cm component. This result disagreed with an earlier less complete observation by Swank and White (1980) where no X-ray eclipse was detected, indicating a much larger scale height for the corona comparable to or greater than the stellar radius. WGB attributed the difference between the two results to flaring activity during the Swank and White observation, although as noted by WGB, unresolved low-level flaring activity could also have distorted their results. These early attempts to measure X-ray eclipses have emphasized that continuous coverage is essential if intrinsic variability is to be distinguished from that caused by eclipses. In this paper we report a continuous observation through the secondary eclipse of Algol using the X-ray detectors on the European X-ray Astronomy Satellite *EXOSAT* (Turner, Smith, and Zimmermann 1982; de

[1] *EXOSAT Observatory*/ESOC, Darmstadt, West Germany.
[2] Affiliated to Astrophysics Division, Space Science Department of ESA.
[3] Mullard Space Science Laboratory, University College London.
[4] Sterrenwacht Sonnenborgh.

Korte *et al.* 1982). The continuous coverage afforded by the 90 hr eccentric *EXOSAT* orbit makes it ideal for eclipse measurements.

Algol is a triple system containing a 70 hr eclipsing binary (K IV and B8 V) in a 694 day orbit with an A V star. The X-ray emission from this system, first observed by Schnopper *et al.* (1976), is thought to be associated with a corona surrounding the lobe filling K IV star. This is based on (*i*) the similarity of the X-ray spectrum and luminosity of this system to that of the RS CVn systems which also contain K subgiants with similar rotation periods (White *et al.* 1980) and (*ii*) the fact that stellar surveys indicate the luminosity of any coronae surrounding the B8 V and AV companion stars to be several orders of magnitude below the observed value of $\sim 10^{30}$ ergs s^{-1} (cf. Pallavicini *et al.* 1981). The close to 90° inclination and similar sizes for the B and K stars (radii of 3.0 $R_\odot$ and 3.4 $R_\odot$, respectively) make Algol an ideal candidate for an eclipse measurement. In addition since the B star is X-ray dark (Pallavicini *et al.* 1981) the complication of two coronal X-ray sources in one system is removed.

In § II an overview of the *EXOSAT* results is given, and in § III a lower limit to the coronal height inferred from the failure to detect any obvious X-ray eclipse. During the observation an 8 hr X-ray flare was seen, and in § IV its spectral evolution is used to estimate the size of flaring region. In § V our conclusions regarding the sizes of the various coronal components in the Algol system are discussed. The principal results of the paper are summarized in § VI. Results of simultaneous radio observations of Algol made at 21 cm are reported by van den Oord *et al.* (1986).

II. THE X-RAY OBSERVATIONS

a) An Overview

The *EXOSAT* observation began at 0900 UT on 1983 August 18 at the quadrature preceeding secondary optical eclipse and continued uninterrupted for one-half of a binary cycle. In Figure 1 the source count rates (with background subtracted) measured by the Medium Energy experiment (ME; Turner, Smith, and Zimmerman 1981) and Low Energy experiment (LEIT; de Korte *et al.* 1981) are shown. The ME experiment consists of an array of proportional counters sensitive in the 1–60 keV band with a total collecting area of 1600 cm^2. Throughout this observation one-half of the array was kept offset from the source to give a continuous monitor of the particle background. The offset array half was periodically alternated to optimize the background subtraction. In quiescence Algol was detected in the 1–8 keV band. The LEIT consists of a Channel Multiplier Array (CMA) at the focus of an imaging telescope. Since the CMA has a UV response it was necessary to interpose an Al/P filter to eliminate the UV contribution giving an effective band pass of 0.05–2.0 keV peaking at ~0.5 keV. Since this is an imaging system, the background rate is very low and was precisely determined from another area of the detector away from the source. A second low

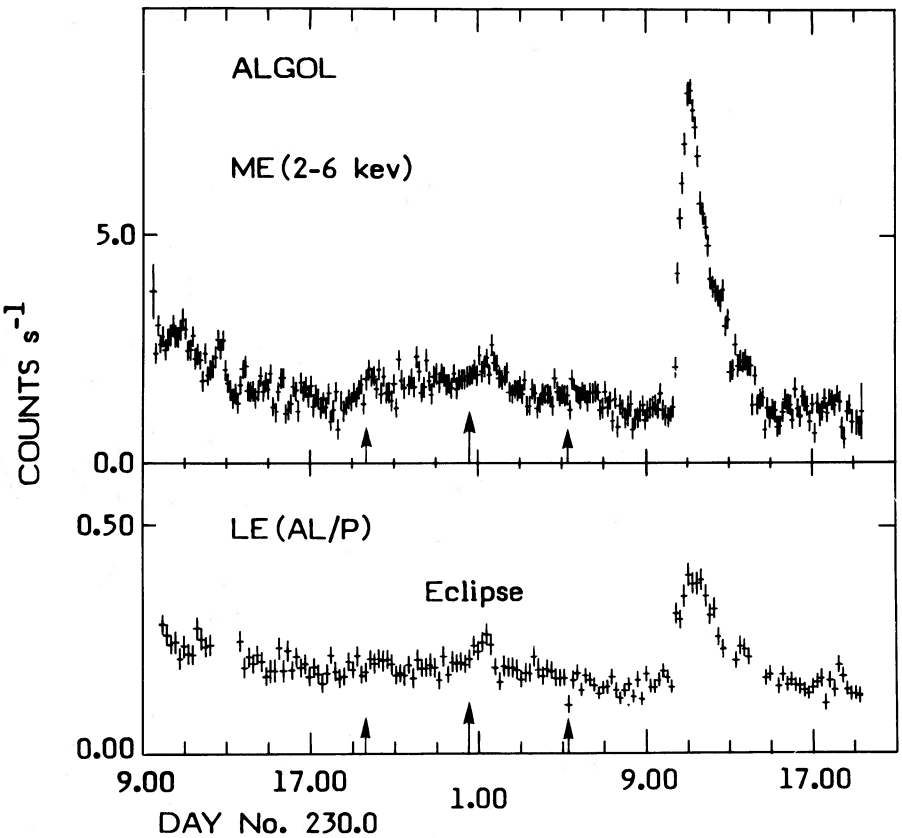

FIG. 1.—Plots of background subtracted intensity against time from the ME and LEIT instruments. The Al/P filter is sensitive in the 0.1–2.0 keV energy band. The time resolution is 10 and 20 minutes in the LEIT and ME, respectively.

Energy Telescope was operated for most of the observation with a 1000 lines mm^{-1} grating interposed in the light path.

The outstanding feature of both the LEIT and ME light curves is an 8 hr flare that occurred at 1300 UT and subsequently decayed exponentially over the following 8 hr. In addition to this event, there is low-level variability in both the ME and LEIT. The continuous background monitoring shows the background to be constant, confirming that the variations are in the X-ray flux. At the start of the observation the count rate decays by a factor of 2 over a few hours, which suggests that another flare may have occurred a few hours earlier. In addition there are other low-level variations of order 20% on a time scale of a few hours. In contrast to this activity there is no clear evidence for any eclipse of the X-ray source between the indicated times of first and last contact (predicted by the ephemeris for primary eclipse JD 2,440,953.4657 + 2.8673075*E*; Ashbrooke 1976).

b) The Spectral Evolution of the Flare

A more detailed light curve of the flare is shown in Figure 2. A hardness ratio obtained from the ME by dividing the 4–6 keV count rate by that between 2 and 4 keV is also plotted. The ME data show that the increase was in two parts; an initial impulsive rise to one third the maximum in 200 s, followed by a more gradual increase to the peak over the following 1500 s. The decay is exponential-like, although 90 minutes after the peak there is a small hump that could be due to a second small flare. The hardness ratio plot shows that during the flare the spectrum becomes harder than the quiescent value, with maximum hardness occurring about 1000 s before flare maximum. The spectrum then softens as the flare progresses. The increase in flux in the LE over the quiescent value is only a factor of ~ 2.5 compared to a factor of ~ 7 in the ME. This again reflects the fact that the flare represents an

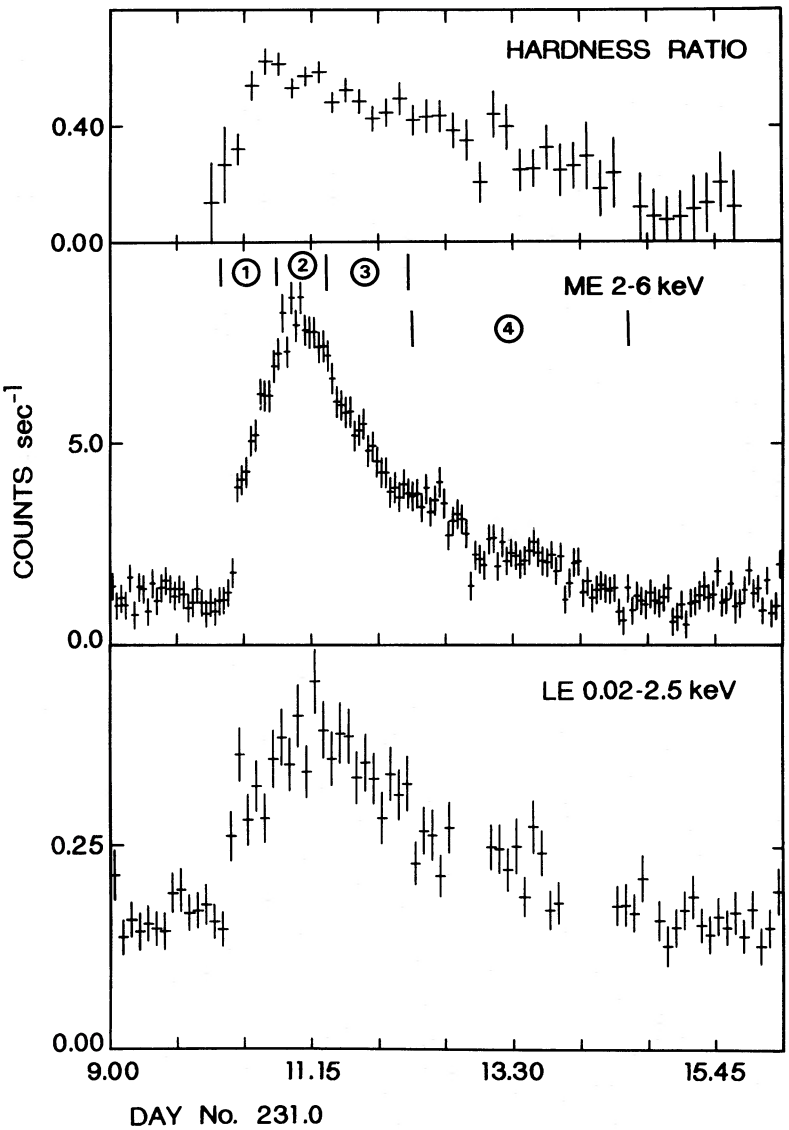

FIG. 2.—A more detailed light curve of the Algol flare shown with a time resolution of 180 s and 360 s in the ME and LEIT, respectively. Also given is a hardness ratio obtained from dividing the ME count rate between 4 and 6 keV by that between 2 and 4 keV. The numbers refer to intervals over which the spectra were accumulated.

overall hardening of the spectrum relative to the quiescent level. There was no evidence for an impulsive spike at higher energies. However, these are in the solar case several hundred times less luminous than the soft X-rays: if this scales the same way for Algol, it would not have been detected in the ME.

Multichannel pulse-height spectra were obtained for the various intervals during the flare, indicated as 1–4 in Figure 2, with the quiescent spectra (that included the quiescent X-ray flux) from either side of the flare subtracted as background. Figure 3 shows the pulse-height spectra from intervals 1, 2 and 3 (Fig. 3*b*–3*d*) with, in addition, the sum of the spectra from all four intervals (Fig. 3*a*). A feature around 6.7 keV that represents Fe XXV line emission broadened by the detector resolution of ~20% is evident in all the spectra, especially in the total spectrum (Fig. 3*a*). A thermal bremsstrahlung plus narrow iron line model convolved through the detector response gave an acceptable fit in all cases and the results are summarized in Table 1. The best fitting models are shown as histograms in Figure 3. The temperature declined over 4 hr from a peak value of 5.0 keV (5.8×10^7 K) to 2.7 keV

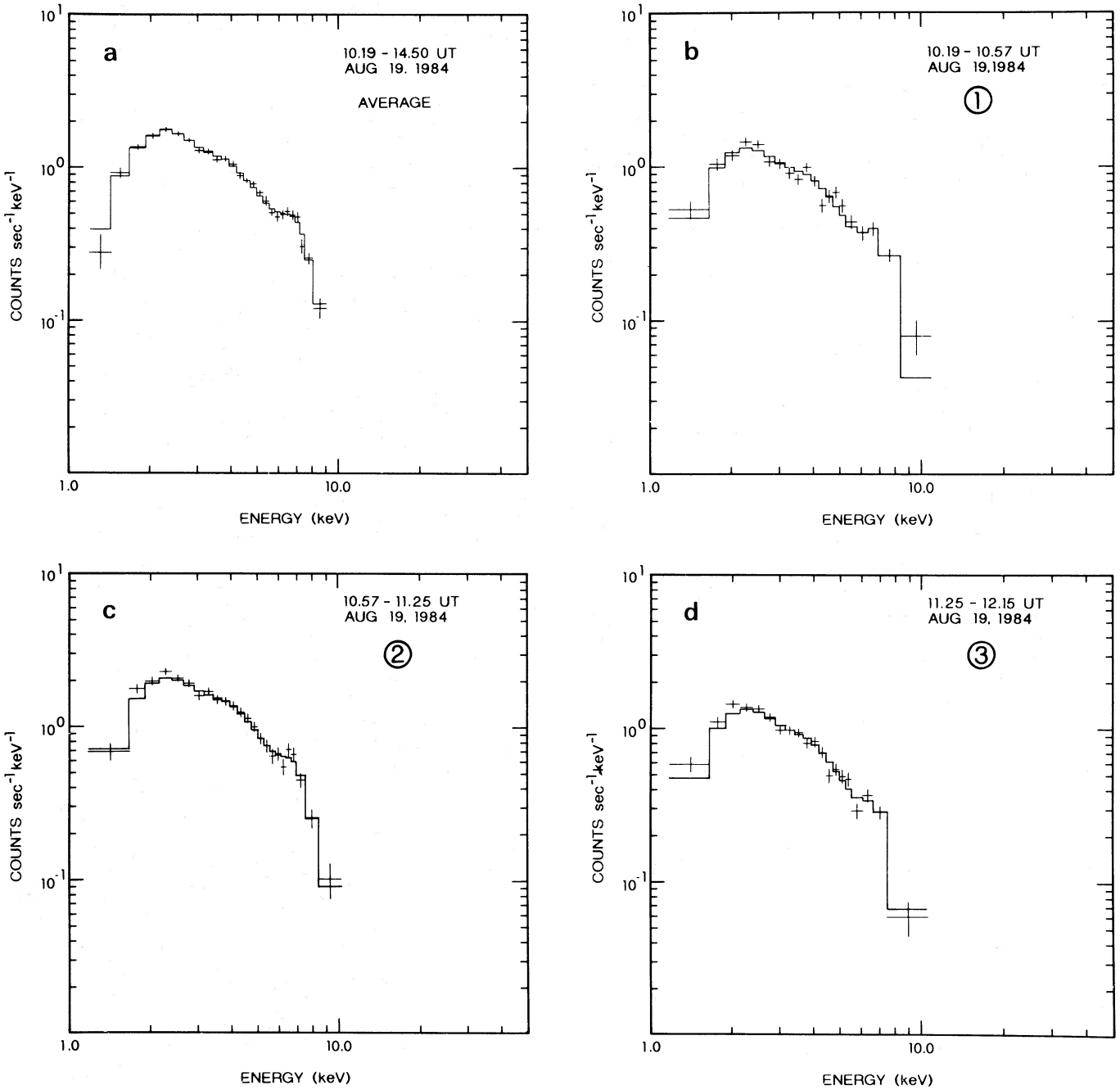

FIG. 3.—Pulse height spectra from the ME for various intervals during the Algol flare. Panel *a* shows the average spectrum of the flare with the best fitting thermal bremsstrahlung model, including an iron line at 6.7 keV. The evolution of the flare spectrum is illustrated in panels *b*, *c*, and *d* using three spectra from the indicated times. The best fitting parameters are given in Table 1.

TABLE 1

SPECTRAL EVOLUTION OF THE ALGOL FLARE[a]

SAMPLE NUMBER	TIME (UT) 1983 Aug 19	kT (keV)	$\int n_e^2 dV$ ($\times 10^{53}$ cm^3)	Fe XXV EMISSION FEATURE: Peak Energy (keV)	Fe XXV EMISSION FEATURE: Equivalent Width (keV)	L_x($\times 10^{30}$ ergs s^{-1})[b]
1.....	10.18–10.57	4.8 ± 0.4	5.8 ± 0.2	7.1 ± 0.2	2.5 ± 0.4	8.5
2.....	10.57–11.25	5.0 ± 0.6	9.4 ± 0.6	6.8 ± 0.2	1.5 ± 0.4	14.0
3.....	11.25–12.15	3.5 ± 0.5	7.0 ± 1.0	6.8 ± 0.2	2.6 ± 0.4	9.4
4.....	12.15–14.30	2.7 ± 0.8	5.7 ± 0.8	6.75 (fixed)	2.3 ± 1.2	6.7

[a] All uncertainties are 1 σ.
[b] For 0.1–10 keV and $d = 27$ pc.

(3.2×10^7 K). The iron line equivalent width was typically ~ 2 keV and its energy ~ 6.8 keV. The measured equivalent widths and line energies are in good agreement with those predicted by Raymond and Smith (1978) from a plasma in ionization-recombination equilibrium for the measured temperature. This confirms the thermal nature of the event and indicates that the iron abundance is within $\sim 20\%$ of the cosmic value (4×10^{-5}).

The emission measure and luminosity are also given in Table 1 for an assumed distance of 27 pc. The peak 0.1–10 keV luminosity was 1.4×10^{31} ergs s^{-1}. The flare emission measure decreased from 9.4×10^{53} to 5.7×10^{53} cm^3 as the flare decayed.

c) *The Quiescent Spectrum*

ME spectra of the quiescent state were obtained for the three intervals corresponding to the two array changes. The duration of the first two are ~ 12 hr, while the third was curtailed to ~ 4 hr by excluding the flare. The times are summarized in Table 2. The data in all three cases are well represented by a thermal bremsstrahlung model with a temperature of ~ 2.1 keV (2.5×10^7 K) and an emission measure of $\sim 5 \times 10^{53}$ cm^{-3}. Two typical spectra are shown in Figure 4 along with the best fitting model. A small excess around 6.7 keV may be due to iron line emission. The inclusion of an iron line is formally required with an equivalent width consistent within the uncertainties with that expected from a solar abundance plasma in ionization equilibrium. However, we note that the line parameters are dependent on systematic uncertainties in the background subtraction and while these results are suggestive of a feature, confirmation is required. These systematic uncertainties are not present in the flare spectra discussed earlier because the background was determined from surrounding data and the flux was much higher. While the temperature of the quiescent spectrum is similar to that of the quiescent high-temperature component found by the *Einstein* SSS, the emission measure deduced from the thermal bremsstrahlung model is somewhat higher.

We have also fitted Raymond and Smith (1978, 1979) and Mewe and Gronenschild (1981) line and continuum models to the data and find similar values of temperature. Because of the contributions of radiative recombination and two-photon continuum, the emission measures required are about 30% lower and are consistent with the values determined from the SSS data.

Using the parameters of the best fitting ME quiescent spectra together with a range of hydrogen column density N_H from 1×10^{17} to 2×10^{18} atoms cm^{-3}, values of the LEIT count rate were predicted. The contribution of the stellar wind of the B star is likely to be comparable to or less than the interstellar value. Count rates corresponding to the maximum and the most likely values of N_H are listed in Table 2 for the various time intervals during the quiescent phase. When these rates are compared with the observed values, it is clear that the extrapolated ME spectra account for between 80% and 100% of the observed counts depending on the assumed value of N_H. While there are substantial uncertainties in N_H, the most probable value is $\sim 1 \times 10^{18}$ H cm^{-2} (Frisch and York 1983). From Table 2, this leads to a prediction of between 85% and 100% of the total LEIT count rate. If we fold the low-temperature emission component ($T_e \approx 7 \times 10^6$ K, $\int N_e^2 dV \approx 1 \times 10^{53}$ cm^3) found by the *Einstein* SSS instrument (White *et al.* 1980; Swank *et al.* 1981) through the LEIT response, we predict an additional LEIT count rate of 0.06 counts s^{-1} or 30% of that observed. This value is insensitive to the uncertainties in the column density and is in excess of what is required, suggesting

TABLE 2

QUIESCENT MEDIUM ENERGY AND LOW ENERGY COUNT RATES[a]

TIME (UT) 1983 Aug 18–19	kT (keV)	$\int n_e^2 dV$ ($\times 10^{53}$ cm^{-3})	Fe XXV LINE EQUIVALENT WIDTH (keV)[b]	L_x[c] ($\times 10^{30}$ ergs s^{-1})	LOW ENERGY COUNT RATE (counts s^{-1}): Observed	Predicted from Extrapolated Medium Energy Spectrum: N_H[d] $= 2 \times 10^{18}$	Predicted from Extrapolated Medium Energy Spectrum: N_H[d] $= 1 \times 10^{18}$
09.30–21.30.....	2.15 ± 0.05	5.5 ± 0.1	1.24 ± 0.5	5.8	0.21 ± 0.002	0.17 (81%)	0.18 (86%)
21.30–08.05.....	2.18 ± 0.05	5.0 ± 0.1	0.6 ± 0.5	5.3	0.18 ± 0.002	0.16 (89%)	0.17 (94%)
15.00–19.20.....	1.95 ± 0.05	4.2 ± 0.1	1.46 ± 0.8	4.1	0.14 ± 0.002	0.13 (93%)	0.14 (100%)

[a] All uncertainties are 1 σ.
[b] Peak energy fixed at 6.75 keV.
[c] For 0.1–10.0 keV and $d = 27$ pc.
[d] Equivalent H atoms per cm^2 column density.

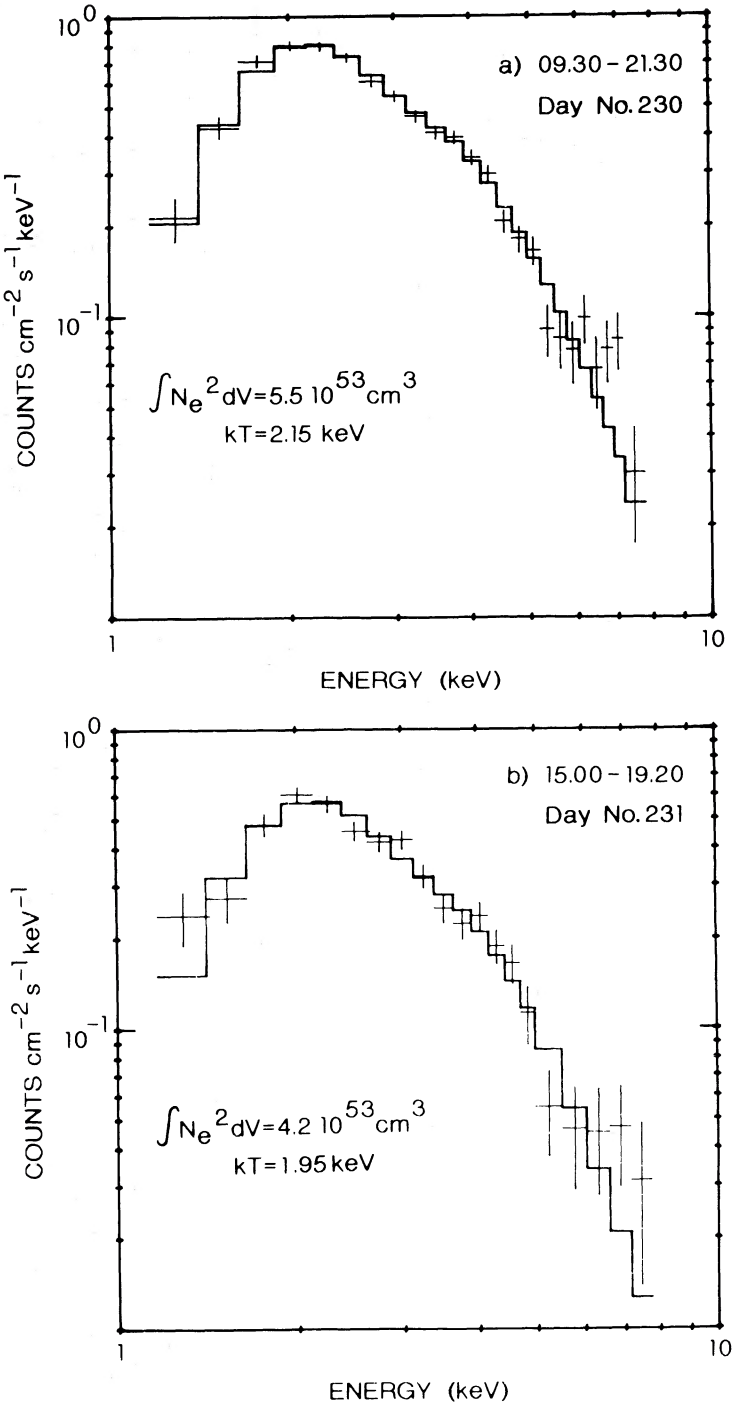

FIG. 4.—The pulse height spectrum obtained from three intervals when the source was quiescent. The best fitting thermal bremsstrahlung model is indicated. The parameters are given in Table 2.

that the emission measure of the low-temperature component was at least a factor of 2 lower during this observation. Thus the count rates in both ME and LEIT are dominated by the contribution of the 2.5×10^7 K component.

The ME data could also be equally well modeled with a power law with a photon index of ~ 2.0 and an $N_H = 6 \times 10^{21}$ H cm^{-2}. However, this model extrapolated into the LEIT would give a factor of 100 larger count rate than observed for $N_H = 1 \times 10^{18}$ H cm^{-2} or a factor of 10 too small for the N_H given by the ME. On this basis we rule out nonthermal models for the >1 keV emission.

Further spectral information can be obtained from the grating data. About 43,000 s total observing time was obtained with the 1000 lines mm^{-1} grating used in combination with a 3000 Å Lexan filter. Unfortunately during the flare an Al/P filter was employed with the grating for a UV calibration

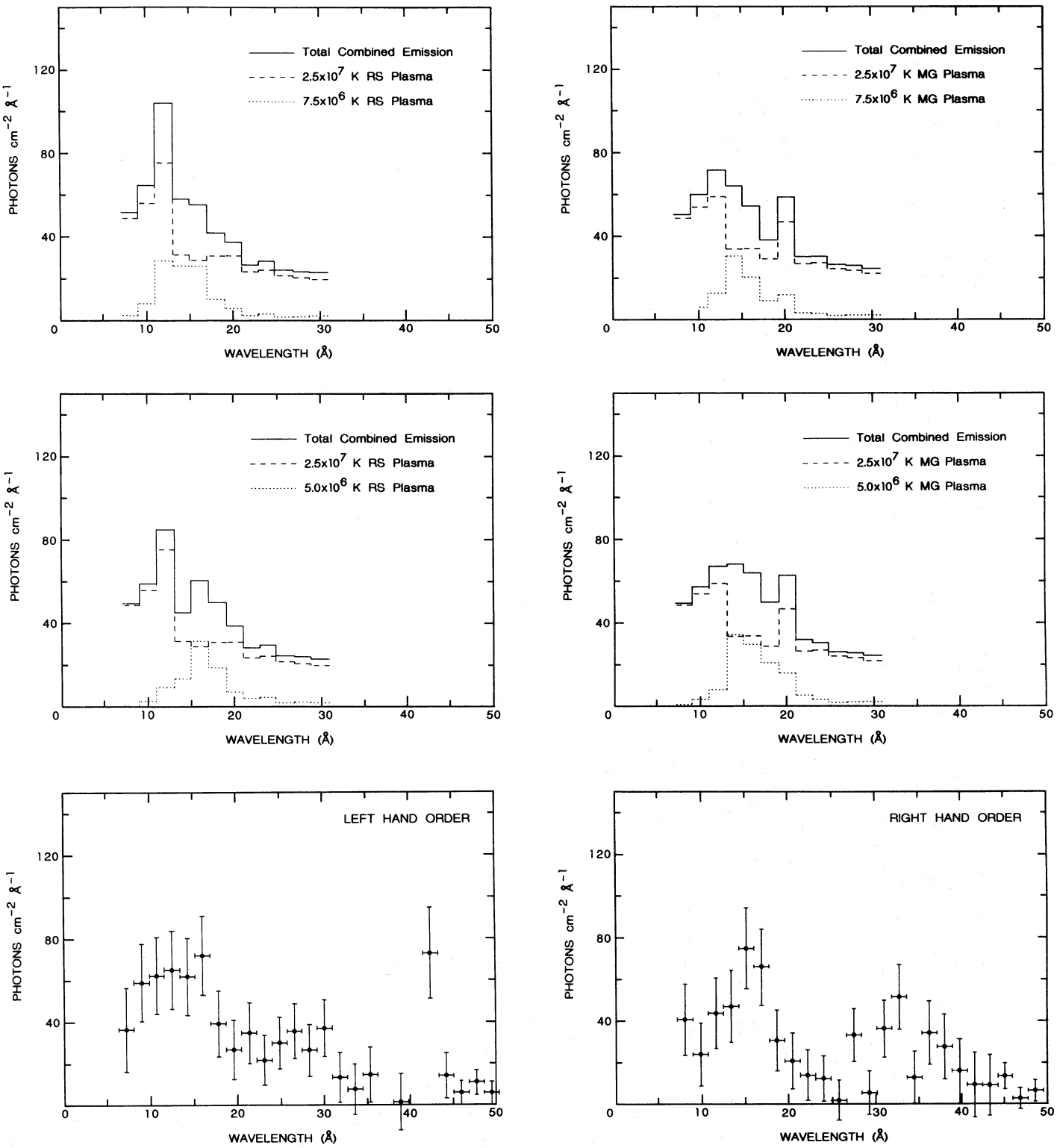

FIG. 5.—Grating spectra obtained during quiescence from the left-hand and right-hand sides of zero order. Also shown are spectral plots corresponding to two-temperature Raymond and Smith (RS) hot plasma models. The higher temperature is that obtained from the ME data. A low-temperature component at 5×10^6 K provides better agreement with the data than a 7.5×10^6 K component.

check, and no useful flare spectra were obtained. The incident spectra obtained from the left and right sides of the grating are shown in Figure 5. Shortward of 7 Å, the grating spectrum is dominated by the zero-order contribution, which was broader than usual because of UV contamination. The background and higher order spectral contribution were subtracted from the raw spectrum, and the result was converted to equivalent photon flux by dividing by the instrument effective area. There is, in both halves, an excess between 10 and 20 Å with evidence for additional low-level emission at longer wavelengths. While the quality of these data is insufficient to constrain the spectrum uniquely, they can be used to check the low-energy extrapolation of the spectrum simultaneously measured by the ME.

In Figure 5 we compare with the data the predicted spectrum for a 2.5×10^7 K plasma with EM = 3.5×10^{53} cm^{-3} from both Raymond and Smith (1978, 1979) and Mewe and Gronenschild (1981). In addition we give for reference the expected contribution from a 5.0×10^6 K plasma with EM = 0.4×10^{53} cm^{-3}. The continuum contribution is plotted separately. The broad feature between 10 and 20 Å is consistent with that expected from the iron L complex. Even at this level the calculations of the strength of this complex are uncertain because of poorly constrained atomic parameters. In particular the calculations of Raymond and Smith (1978, 1979) give a much stronger feature at 12 Å than those of Mewe and Gronenschild or than is evident in the data themselves. However, overall the grating data is consistent with the spectrum measured by the ME. Any contribution from the 5.0×10^6 K component would be confined to iron L emission around 15 Å. The centroid and contribution of the emission is very sensitive to the an assumed temperature and since the SSS measurement was dominated by this emission, the uncertainty in its contribution is dominated by that in the atomic physics.

III. THE ECLIPSE

It is apparent from the LEIT and ME light curves that there is no significant decrease in the observed flux at the predicted times of eclipse. However a limit placed on any possible eclipse can still be used to constrain models of the K star coronal structure associated with the 2.5×10^7 K component (but not the 7×10^6 K component) for an assumed coronal geometry.

The K star corona was modeled as a spherically symmetric exponential atmosphere, characterized by a scale height, R_0. The eclipse model included the radii of the K and B stars, along with the orbital inclination and semimajor axis of the Algol AB binary system. The assumed values were $R_K = 3.5R_0$, $R_B = 2.9R_0$, $i = 82°.3$, and $R_{AB} = 13.97R_0$ (Soderhjelm 1980). This model was then used to predict the expected X-ray light curve produced by the passage of the X-ray–dark B star across the X-ray–emitting K star corona. When the coronal scale height is large compared to the stellar radius, the corona shows strong limb brightening such that *two* minima should occur, symmetrically, either side of mid-eclipse (Fig. 6 [*top*]). Figure 6 (*center*) gives the predicted depth of the eclipse minima (normalized to 1.0 outside eclipse) as a function of R_0, the scale height of the K star atmosphere.

The ME light curve can now be used to place limits on the size of the K star corona associated with the high-temperature component. Due to the source being quite weak in the ME and the somewhat variable nature of the Algol during this observation, we can only place a $\sim 10\%$ limit on any possible eclipse "dips" going unobserved. This sets a lower limit of about $3R_0$ (or ~ 1 stellar radius, R_*) to the scale height of the K star atmosphere.

However, just *before* first contact, and just *after* fourth contact, there are two small dips (Fig. 6 [*bottom*]). When analyzed individually, they indicate 20%–30% reduction in the ME flux. While recognizing that these two features may represent random fluctuations in the source intensity, their approximate symmetry about the time of mid-eclipse is notable. The simple eclipse model discussed earlier predicts minimum light to occur just *after/before* first/fourth contact, due to the strong limb brightening of the corona in the model. These features then occur *early and late* with respect to the model predictions. If these dips are real, they are caused by the obscuration of X-ray bright features in the K star corona that are well above the surface of the star: probably large coronal loop structures.

IV. THE SIZE OF THE FLARING REGION

The observation of giant stellar X-ray flares with luminosities of $\sim 10^{31}$ ergs s^{-1} is now a relatively common phenomenon of RS CVn and related systems (White, Sanford, and Weiler 1978; Garcia *et al.* 1980; Schwartz *et al.* 1981; McHardy *et al.* 1982; Pye and McHardy 1983, Stern, Underwood, and Antiochos 1983). For the flare we have observed from Algol, the continuous spectral and temporal coverage achieved represents a marked improvement over earlier observations. The impulsive rise, subsequent extended rise and then long decay over 8 hr is reminiscent of the behavior seen in solar "two-ribbon" flares. However the peak X-ray luminosity is more than two orders of magnitude greater than that of the largest solar events and three orders of magnitude greater than a stellar flare from Proxima Centauri that Haisch *et al.* (1983) classified as two-ribbon. Nonetheless the thermal character of the flare typified by the Fe XXV emission seen by the ME strongly suggests that, as in the solar case, the flare is caused by the heating of a solar abundance thermal X-ray plasma. By analogy with the solar example we will assume that the plasma is confined by a magnetic loop or loops anchored to the chromosphere of the K subgiant. If the X-ray heating phase ends at flare maximum and the volume containing the plasma remains constant, then the plasma will cool by radiation and/or conduction (Culhane, Vesecky, and Phillips 1970; Moore *et al.* 1980; Haisch 1983).

We will consider two different possibilities: (*i*) radiation cooling dominates, and (*ii*) conduction cooling dominates. In both causes we assume the X-ray plasma to be contained in N_L loops of length L with a height H above the stellar surface of L/π and a radius of αH, where α is the ratio of the loop radius to its height (typically 0.1 in the solar case). The emission measure is then given by:

$$\int n_e^2 dV = n_e^2 \pi^2 H^3 \alpha^2 N_L \text{ cm}^{-3} , \quad (1)$$

with $\alpha^2 N_L$ expressing our uncertainty in the loop geometry.

i) *Radiation Cooling*

The time scale for radiation cooling τ_r is given by

$$\tau_r = \frac{3kT_p}{n_e \Lambda} \text{ s} , \quad (2)$$

where T_p is the peak temperature, n_e is the density, and Λ is the

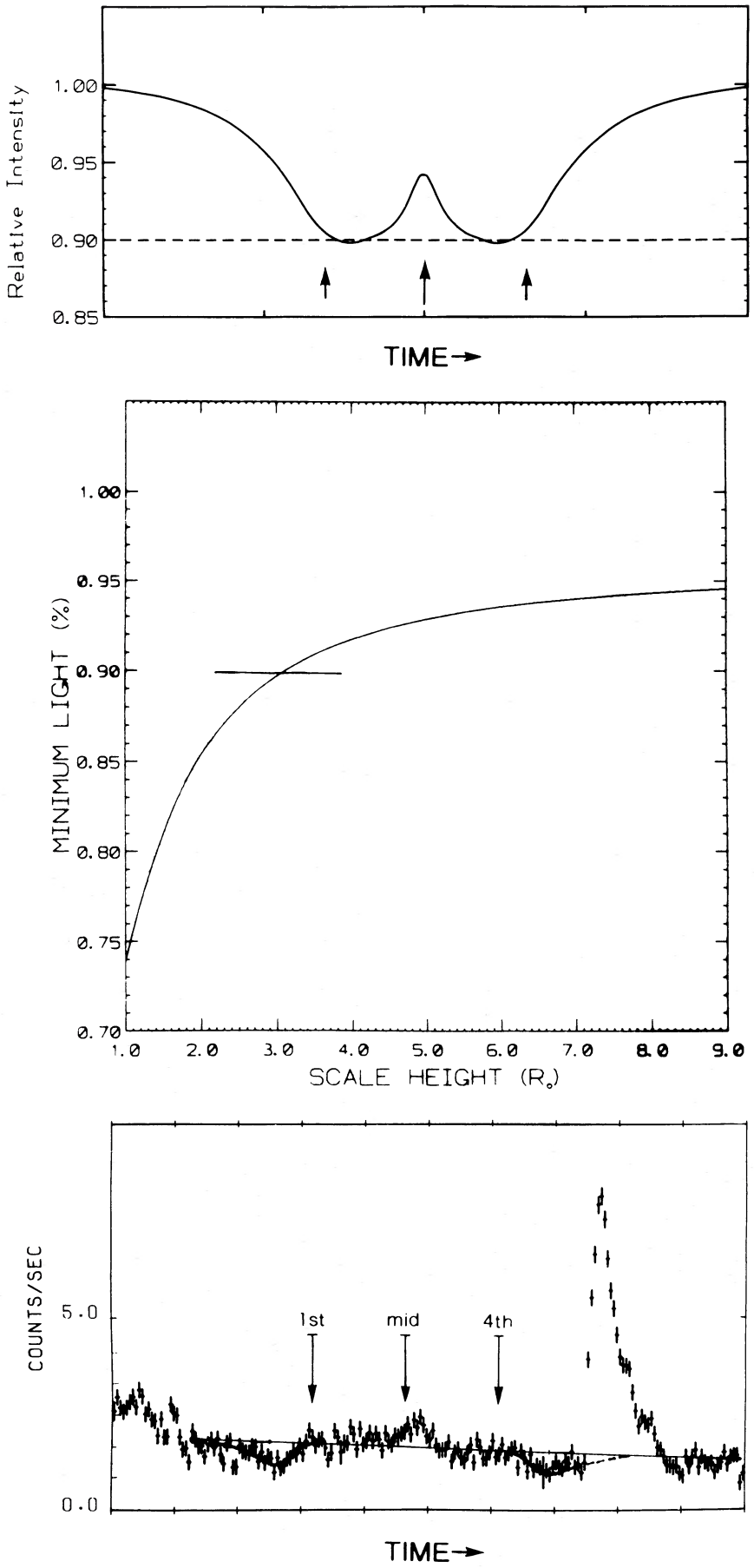

FIG. 6.—(*top*) Results of a simulated eclipse of the K star with a spherically symmetric exponential atmosphere with a scale height of 3 $R_{\odot}$. Coronal limb brightening leads to two pronounced minima on either side of mid-eclipse. (*center*) The fractional depth of the predicted minima as a function of the scale height of the corona. (*bottom*) The Algol ME light curve with possible eclipses of localized coronal structures before first contact and after fourth contact.

radiative loss function, which for the observed temperature range of 5.8×10^7 K to 3.2×10^7 K is $10^{-26.8} T_p^{0.5}$ ergs cm^{-3} s^{-1}. This can be equated to the observed exponential decay time (Fig. 2) of $\tau_d \approx 7000$ s to give $n_e = 3 \times 10^{11}$ cm^{-3} for $T_p = 5.8 \times 10^7$ K. Combining this density estimate with the peak emission measure of 9×10^{53} cm^{-3} gives a volume of 1×10^{31} cm^3. From this we obtain

$$H = 5 \times 10^{10} (\alpha_{0.1}{}^2 N_L)^{-1/3} \text{ cm} . \quad (3)$$

ii) *Conduction Cooling*

For a coefficient of conductivity of $8.8 \times 10^{-7} T^{-2.5}$ ergs s^{-1} cm^{-2} K^{-1} (Spitzer 1962) the time scale for conductive cooling, τ_c is given by

$$\tau_c \approx 1.18 \times 10^{-10} n_e L^2 / T_e^{2.5} \text{ s} \quad (4)$$

(Culhane, Vesecky, and Phillips 1970). Using equation (1) with $\int n_e{}^2 dV = 9 \times 10^{53}$ cm^{-3} to eliminate n_e from equation (4) gives

$$H = 2.5 \times 10^9 \alpha_{0.1}{}^2 N_L \text{ cm} . \quad (5)$$

An additional constraint on H is provided by the fact that radiation cooling depends only on density, whereas the conduction is a function of both density and loop length. For the conduction heat loss to become comparable to, or greater than, that of radiation requires that $n_e < 3 \times 10^{11}$ cm^{-3}. This effectively sets a lower limit to H of 2×10^{10} cm. Conductivity can be inhibited by up to a factor of 10 by constriction of the loop legs (Antiochos and Sturrock 1978) such that the derived values of H can be lower by up to a factor of 100.

In both cases the height of the loop is dependent on $\alpha_{0.1}{}^2 N_L$, and in Figure 7 we show how H varies in terms of these parameters, for the two possibilities. The two lines intersect at the point where $\tau_c = \tau_r$. This defines a *minimum* height for the loop. The case when conductivity is inhibited by a factor of 10 is shown with dashed lines. When conduction dominates the cooling ($\tau_r \gg \tau_c$) there is no valid solution for $\alpha_{0.1}{}^2 N_L < 10$. Thus unless $\alpha_{0.1} > 3$, which seems unlikely, the flare plasma must in this case be contained in 10–100 loops with height of between 0.1 to 1.0 R_* flaring in concert with a plasma density $\ll 10^{11}$ cm^{-3}. While in the solar case a flare in one loop may cause an adjacent loop to flare, multiple flares occupying 10 or more loops are not seen. Thus based on the solar analogy we consider this possibility unlikely. For $\tau_r \ll \tau_c$ and $\alpha_{0.1}{}^2 N_L < 10$, the range of loop height is restricted still further to $2 \times 10^{10} < H < 5 \times 10^{10}$ cm ($0.09\ R_* < H < 0.21\ R_*$), where R_* is the stellar radius.

The linear decline in the hardness ratio and temperature (Fig. 2 and Table 1) suggests additional heating may have occurred well into the flare decay, as occurs in two-ribbon flares (Moore *et al.* 1980). There is some evidence for a small reenergization of the flare at $\sim$1245 UT which may in part be responsible for this effect. However, the density and volume inferred from the radiative cooling time give a total available energy of $\sim 1 \times 10^{35}$ ergs s^{-1} which is indeed comparable to the integrated luminosity for the flare (Table 1), suggesting that the effects of additional heating are small.

For magnetic containment, the gas pressure at flare maximum of 3200 dyn must not exceed $B^2/8\pi$, which gives $B > 200$ G. This gives a lower limit to the preflare Alfvén velocity, v_A, for a given preflare coronal density. If the coronal density did not *decrease* during the flare, then $v_A > 3.10^7$ cm s^{-1}. This velocity should, within an order of magnitude, represent the propagation velocity of the magnetic instability responsible for the flare, such that the flare rise time will be comparable to L/v_A. The range of H derived for $\tau_c > \tau_r$ leads to

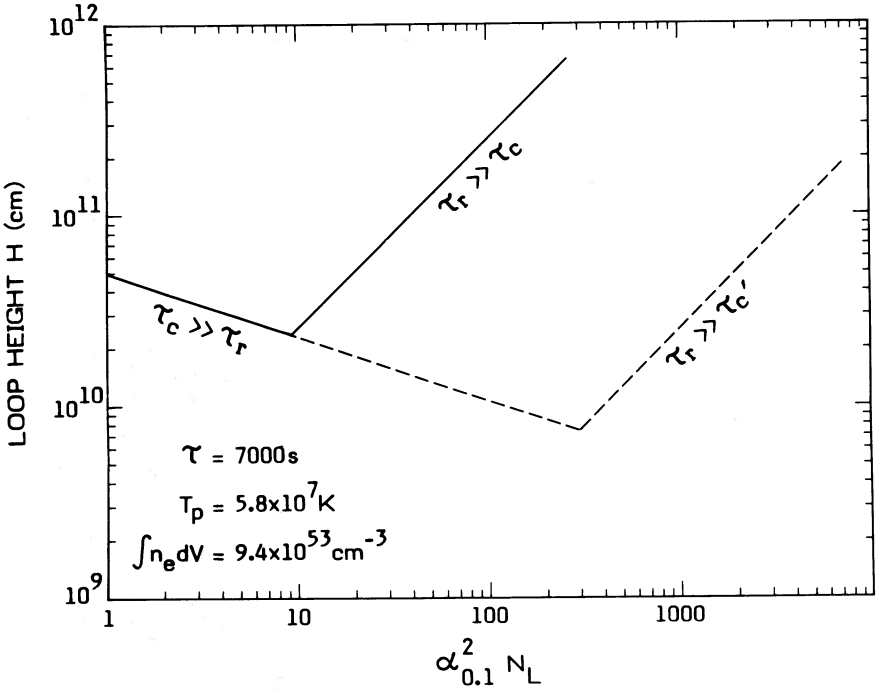

FIG. 7.—For a cooling plasma contained in N_L loops with a radius to height ratio α, the loop height, H, is shown as a function of $\alpha_{0.1}^2 \times N_L$ for the regions when (*i*) radiation cooling dominates and (*ii*) conduction cooling dominates. The dashed lines represent the case where conduction is inhibited by up to a factor of 10 by constriction of the loop leg. A peak emission measure of 9.4×10^{53} cm^{-3}, a temperature of 5×10^7 K, and flare decay time of 7000 s were assumed.

a rise time of < 5000 s, quite consistent with the observed value of 1700 s.

V. DISCUSSION

The failure to detect any clear X-ray eclipse at the time of secondary eclipse demonstrates that if the 2.5×10^7 K X-ray emission is associated with a corona surrounding the K IV secondary, then its scale height must be comparable to or greater than that of the underlying star. There does not seem to be any plausible alternative to this conclusion. The two other stars in this triple system are both of a much earlier spectral type and, based on the stellar X-ray survey presented in Pallavicini *et al.* (1982*a*), any corona associated with either of them should be many orders of magnitude less luminous than is observed. The model put forward by Harnden *et al.* (1978) that the X-rays come from shock heated material at the impact point on the B star of the gas stream from the K star is also ruled out since the impact point was self occulted by the B star for most of this observation. Because the thermal energy of the 2.5×10^7 K plasma exceeds the surface gravitational potential energy of the K IV star, magnetic confinement is essential.

The total loop volume available, V, can be expressed in terms of f, the fraction of the star covered in loops as $V = \pi^2 R_*^2 f H$ for a loop geometry, where the cross section of the loop is constant along its length. The pressure, P, of the plasma contained in the loop is then given by

$$P = \frac{4.6\ \mathrm{EM}_{53}{}^{0.5} T_7^{0.5}}{H_*{}^{0.5} f^{0.5}}\ \mathrm{dyn\ cm^{-2}}\ .$$

In Figure 8 the variation of P with H is shown for a variety of f. As the loop height increases to stellar dimensions the volume behind the star becomes visible and f can exceed unity. If the loop cross section increases with height then P will decrease more rapidly (cf. Swank *et al.* 1981). This can be approximated by making f greater than 2. From Figure 8 it is apparent that loop pressures in excess of about 100 dyn cm^{-2} will be required if the plasma is to be contained in typical solar-sized loops ($H \approx 0.01$–$0.05\ R_*$). For a more reasonable range of pressure of $\sim$1–10 dyn, closer to that indicated by UV observations of transition region lines in RS CVn systems (e.g., Simon and Linsky, 1980), the loop heights are comparable to the binary separation. This is independent of any assumed scaling law that relates the temperature and pressure of the contained plasma to the loop length.

Application of the Rosner-Tucker-Vaiana (RTV) scaling relation gives similarly large loop scale heights for the observed temperatures and transition region pressures (cf. Simon and Linsky 1980). In Figure 8 we plot the RTV relation for the 2.5×10^7 K component. When $f > 1$ the solution gives loop pressures of < 20 dyn cm^{-2} and scale heights greater than a stellar radius. If $f < 1$ then the loop pressure exceeds 100 dyn cm^{-2} and the loop height $H < 0.1\ R_*$. Thus we are again left with two possibilities: solar-sized, high-pressure loops or stellar-sized lower pressure loops. In the latter case the high f values require that the loop cross section strongly increases with height (cf. Swank *et al.* 1981). The failure to detect any clear eclipse of the > 1 keV emission directly demonstrates that the latter solution is the correct one.

When the flare is modeled in terms of a magnetically confined cooling plasma, the loop height is $\sim$0.1–0.2 R_* if radiation cooling dominates over conduction. The loop size can only be greater than a stellar radius when conduction dominates. However this requires that the flare was contained in hundreds of loops flaring in concert, which seems unlikely. The loop heights of $\sim$0.1–0.2 R_* do not necessarily conflict with the large scale height derived from the failure to detect an X-ray eclipse. By analogy with the Sun a range of loop sizes is to be expected. The *Einstein* SSS results also required the pre-

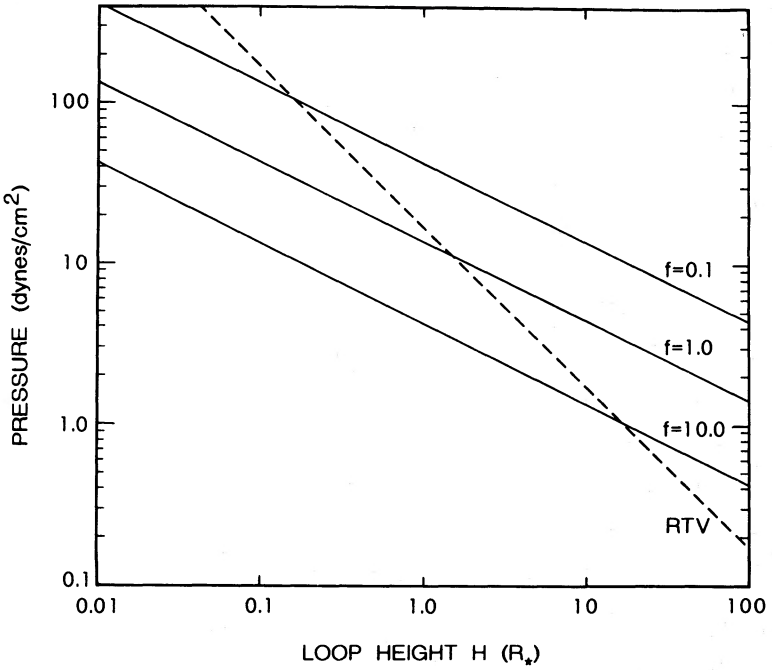

FIG. 8.—The relationship between loop pressure and height for the measured quiescent temperature of 2.5×10^7 K and emission measure of 5.0×10^{53} cm^{-3}, when different covering fractions, f, are assumed. Values of f greater than 2 require loop cross sections that increase with height. Also shown is the scaling relation of Rosner, Tucker, and Vaiana (1978).

TABLE 3

FLARE PROPERTIES FOR THE SUN AND ALGOL

PARAMETER	TYPICAL SOLAR		ALGOL (1983 Aug)
	Compact	Two-Ribbon	
$L_{x\,(TOT)}$ (ergs)	10^{30}–10^{31}	10^{32}	10^{35}
Rise time (s)	10^2	10^3	2×10^3
Decay time (s)	10^3	10^4	7×10^3
Peak temperature (10^7 K)	2–3	2–3	6
Peak n_e	10^{11}–10^{12}	10^{10}–10^{11}	3×10^{11}
Peak volume (cm^3)	10^{26}	10^{29}	1×10^{31}
Height of loop (km)	10^3–2×10^4	10^5	2–5×10^5
Loop magnetic field (G)	>100	>100	>200

sence of a lower temperature component ($\sim 5 \times 10^6$ K) with an emission measure of $\sim 10^{53}$ cm^3. The dimensions of this component can, for loop pressures of <100 dyn, be less than a stellar radius and comparable to that inferred here from the flare modeling. Because Algol is a bright UV object the filter interposed in the LEIT to eliminate UV contamination (Al/P) also substantially reduced the sensitivity to the low temperature component. This component contributed <20% of the total count rate in the LEIT, and the eclipse measurement did not provide any constraint on its dimensions.

The *Einstein* IPC eclipse measurement of AR Lac by WGB supports the view that any $< 7 \times 10^6$ K emission comes from more compact loops, with eclipse features in the X-ray light curve giving scale heights between 0.02 and 1.0 R_*. At most only 50% of the *Einstein* IPC count rate would originate from the 2×10^7 K component. Since the count rate in the SSS was dominated by the hotter component, then if in AR Lac the 2×10^7 K component were from a region larger than a stellar radius, this would explain why the *Einstein* SSS observation failed to detect an eclipse. An *EXOSAT* observation of AR Lac around one binary cycle, to be reported in detail elsewhere, confirms this scenario.

VI. CONCLUSIONS

In analyzing the data obtained, we have used two independent methods to determine the size of the coronal structures surrounding the K IV secondary in the Algol system. First, the eclipse observation failed to detect any major reduction in flux, suggesting that the >1 keV emission comes from loop structures with dimensions comparable to or larger than the dimensions of the underlying star. Second, the detection of a large flare allowed the dimensions of the loop containing the flare plasma to be determined for an assumed cooling law. The only plausible solution is for radiation cooling dominating during the flare decay and this yielded a loop height of ~ 0.1–0.2 R_*. This suggests that the flare occurred in a loop that in quiescence, contains plasma that has a temperature less than 10^7 K and so was not detectable during the eclipse. Such a range of loop sizes is hardly surprising. The observed emission measures for the 2.5×10^7 K emission, when combined with the lower limit to the coronal size given by the failure to detect an eclipse, gives loop pressures of order a few dynes cm^{-2}, comparable to those found from UV measurements of transition region lines and comparable to the solar values. This suggests that as the length of a loop increases, the temperature of the contained plasma also increases.

While the height of the flaring loop responsible for the Algol flare is smaller than that causing the bulk of the quiescent >1.0 keV emission, it is still large when compared to typical solar active regions. In Table 3 the properties of the Algol flare are compared with those of two-ribbon and compact solar events (taken from Moore *et al.* 1980) assuming, for the Algol event, a single loop with radiation-dominated cooling. The derived density of $\sim 10^{11}$ cm^{-3} is typical of both types of solar event, but the volume was two orders of magnitude larger than that of a two-ribbon event. However, the peak luminosity was still an order of magnitude below the maximum previously detected from other RS CVn systems (cf. Pye and McHardy 1983). Thus it seems reasonable to assume that these most luminous events originate in the stellar system–sized loop complexes (cf. Simon, Linsky, and Schiffer 1980).

We thank Jean Swank for a critique of an earlier version of this manuscript.

REFERENCES

Antiochos, S. K., and Sturrock, P. A. 1978, *Ap. J.*, **220**, 1127.
Ashbrooke, J. 1976, *Sky and Tel.*, **52**, 48.
Culhane, J. L., Vesecky, J. L., and Phillips, K. J. H. 1970, *Solar Phys.*, **15**, 394.
de Korte, P. A. J., *et al.* 1981, *Space Sci. Rev.*, **30**, 495.
Frisch, P. C., and York, D. G. 1983, *Ap. J. (Letters)*, **271**, L59.
Garcia, M., Baliunas, S. L., Conroy, M., Johnston, M. D., Ralph, E., Roberts, W., Schwartz, D. A., and Tonry, J. 1980, *Ap. J. (Letters)*, **240**, L167.
Haisch, B. M. 1983, in *IAU Colloquium 71, Activity in Red-Dwarf Stars*, ed. P. B. Byrne and M. Rodono (Dordrecht: Reidel), p. 255.
Haisch, B. M., Linsky, J. L., Bornmann, P. L., Stencel, R. E., Antiochos, S. K., Golub, L., and Vaiana, G. S. 1983, *Ap. J.*, **269**, 280.
Harnden, F. R., Fabricant, D., Topka, K., Flannery, C. P., Tucker, W. H., and Gorenstein, P. 1977, *Ap. J.*, **214**, 418.
Holt, S. S., White, N. E., Becker, R. H., Boldt, E. A., Mushotzky, R. F., Serlemitsos, P. J., and Smith, B. W. 1979, *Ap. J. (Letters)*, **234**, L65.
McHardy, I. M., Pye, J. P., Fairall, A. P., Caldwell, J. A. R., and Spencer-Jones, J. H. 1982, *M.N.R.A.S.*, **201**, 31P.
Mewe, R., and Gronenschild, E. H. B. M. 1981, *Astr. Ap. Suppl.*, **45**, 11.
Moore, R. L., *et al.* 1980, in *Solar Flares*, ed. P. Sturrock (Boulder: Colorado Associated University Press), chap. 8.
Pallavicini, R., Golub, L., Rosner, R., Vaiana, G. S., Ayres, T., and Linsky, J. L. 1981, *Ap. J.*, **248**, 279.
Pye, J. P., and McHardy, I. M. 1983, *M.N.R.A.S.*, **205**, 875.
Raymond, J., and Smith, B. 1978, *Ap. J. Suppl.*, **35**, 419.
———. 1979, private communication.
Rosner, R., Tucker, W. H., and Vaiana, G. S. 1978, *Ap. J.*, **220**, 643.
Schnopper, H. W., Delvaille, J. P., Epstein, A., Heimken, H., Murray, S. S., Clark, G., Jernigan, G., and Doxsey, R. 1976, *Ap. J. (Letters)*, **210**, L75.
Schwartz, D. A., Garcia, M., Ralph, E., Doxsey, R. E., Johnson, M. D., Lawrence, A., McHardy, I. M., and Pye, J. P. 1981, *M.N.R.A.S.*, **196**, 95.

Simon, T., and Linsky, J. L. 1980, *Ap. J.*, **241**, 759.
Simon, T., Linsky, J. L., and Schiffer, F. H. 1980, *Ap. J.*, **239**, 911.
Soderhjelm, S. 1980, *Astr. Ap.*, **89**, 100.
Spitzer, L. 1962, *Physics of Fully Ionized Gases* (2d ed.; New York: Wiley Interscience).
Stern, R. A., Underwood, J. H., and Antiochos, S. K. 1983, *Ap. J.* (*Letters*), **264**, L55.
Swank, J. H., and White, N. E. 1980, in *Cool Stars, Stellar Systems, and the Sun*, ed. A. Dupree (Cambridge: Smithsonian Astrophysical Observatory).
Swank, J. H., White, N. E., Holt, S. S., and Becker, R. H. 1981, *Ap. J.*, **246**, 208.
Taylor, B. G., Andresen, R. D., Peacock, A., and Zobl, R. 1984, *Space Sci. Rev.*, **30**, 479.
Turner, M. J. L., Smith, A., and Zimmermann, H. V. 1981, *Space Sci. Rev.*, **30**, 513.
van den Oord, G. H. J., Kuijpers, J., White, N. E., van de Hulst, J. M., and Culhane, J. L. 1986, *Astr. Ap.*, submitted.
Walter, F. M., and Bowyer, S. 1981, *Ap. J.*, **245**, 671.
Walter, F. M., Gibson, D. M., and Basri, G. S. 1983, *Ap. J.*, **267**, 665 (WGB).
White, N. E., Holt, S. S., Becker, R. H., Boldt, E. A., and Serlemitsos, P. J. 1980, *Ap. J.* (*Letters*), **239**, L69.
White, N. E., Sanford, P. W., and Weiler, E. J. 1978, *Nature*, **274**, 569.

A. N. PARMAR and N. E. WHITE: *EXOSAT* Observatory/ESOC, Robert Bosch Strasse 5, 61 Darmstadt, West Germany

J. L. CULHANE, S. KAHN, and B. J. KELLETT: Mullard Space Science Laboratory, Department of Physics and Astronomy, University College London, Holmbury St. Mary, Dorking, Surrey, UK

J. KUIJPERS and G. H. J. VAN DEN OORD: Sterrenwacht Sonnenborgh, Zonnenburg 2, 3512 NL Utrecht, The Netherlands